

## ELECTROMECHANICAL AND RF INVESTIGATIONS OF FIXED-FIXED CONFIGURATION-BASED RF MEMS SWITCH

M.S.G.Prasad<sup>1</sup>, G.V.Ganesh<sup>1</sup>, S.Nagendram<sup>1</sup>, B.Venkat<sup>1</sup>, S.Manogna<sup>1</sup>, Bh.Niharika<sup>1</sup>

<sup>1</sup>Department of Electronics and Communication Engineering, Koneru Lakshmaiah Education Foundation, Vaddeswaram, AP, India.

Received: 15.11.2019

Revised: 20.12.2019

Accepted: 25.01.2020

### Abstract

A shunt type RF MEMS switch design and analysis are presented in this paper for tunable applications. Switch operations are based on the principle of electrostatic actuation. The electromechanical and electromagnetic simulation tests were contrasted with the hypothetical measured switch parameters. The effect of different materials such as conductor and dielectrics & parameters such as air gap, beam width on the switch's electromechanical parameters is analyzed to obtain low pull-in voltage, high switching speed, better capacitance ratio, return loss, insertion loss, and insulation loss. The condition capacitance of the turn up and down is 40.9fF and 4.45pF respectively. The switch's down to state capacity ratio is 108.69. The designed switch has a 32V voltage of actuation. Simulation of RF output from 1-10GHz. The return loss in the ON state shift (switch) is -35dB, the insertion loss is -0.1dB. There is a return loss of -1dB in the OFF-state switch and a loss of -11dB in isolation.

**Key words:** RF MEMS switch, electrostatic actuation, tunable application, insulation loss, insertion loss, switching speed.

© 2019 by Advance Scientific Research. This is an open-access article under the CC BY license (<http://creativecommons.org/licenses/by/4.0/>)  
DOI: <http://dx.doi.org/10.31838/jcr.07.02.63>

### INTRODUCTION

In the past few years, there has been a huge development in the area of communication. Communication of the subsequent generation involves bandwidth, high linearity and low power consumption devices [1]. In communication applications, the choice of RF MEMS switches is to substitute traditional switches. Satellite connectivity was typically used in the phased radar array. The conventional RF MEMS switch uses high-performance silicone as the basis for the coplanar waveguide signal transmission. As a shift command, the central beam structure is used. When the beam comes into contact with the insulating layer, the switcher is disabled, and the signal is blocked on the transfer line for close operation. Due to their advantages, switches gain attention among all MEMS devices the benefits of such the power consumption of switches is extremely poor over other switch types like pin diodes and FET switches [2], because of a low power consumption, device costs are reduced, and performance improves. Super strong insulation, quite small loss of insertion, compact system size, so the circuit width is small. MEMS device manufacturing techniques are the same as microelectronic circuits based on silicon, these are also produced by micromachining techniques for the bulk and surface. A number of RF MEMS switches have been designed and manufactured over the past few years. Many capacitive shunt switches are recorded in the literature with good actuation voltage, loss of insertion and loss of return. The applications include VCOs, phase transformers, filters, amplifiers, condenser banks, etc. During this procedure, optimized geometric parameters have been selected to change, one shunt and the other series. Afterwards we use HFSS to evaluate RF efficiency.

### RF MEMS Switch Design:

The switch is a parallel capacitor of RF MEMS. The entire shift, which is the metal-dielectric sandwich structure, is subdivided into three layers from top to down. The choice of the metal beam material is crucial in order to minimize the actuating voltage of the switch. Gold, with a relatively high modulus and a low residual pressure, is used as the switch beam in this article. The voltage can be cancelled, and the original location can be restored easily. Gold also has a small skin depth which affects the signal transmission very little at the same time. The switch

has a coplanar waveguide design, on the one hand the bracelet supports the beam's two sides, it is possible to stabilize the metal beam structure; on the other hand, it is possible to reduce the switch's degree of insulation. The projection of the switch crosses the line of the signal. Between the beam and signal line, there is an isolating surface that can prevent the direct beam-to-signal line communication. The actuating power applied by electrostatic force and deformation to the central part of the beam resulting in a condenser by touching the isolating surface, Signal transmission through firearms to the ground to block the signal.

### RF MEMS switch analysis:

The plate's actuation voltage is especially important in the switch's design process. Typically, the switches are powered by a DC voltage that curves the metal beam and then maintains balance with the elasticity of the metal beam. The metal beam is conditioned by a static force between the fall electrode and the switch beam when the activation voltage is applied between the beam and the pull-down electrode.

### Switch and Analytical Suggestions:

The layout of the shunt shift suggested is at the bottom. The substratum is 20 μm thick silicon (11.68 dielectric constant). A SiO<sub>2</sub> oxide layer (dielectric constant 3.9) with a thickness of 15 μm is mounted on top of the substratum. On the anchors of the ground line there is a steel layer placed on the signal line of the coplanar waveguide (CPW). A 220 nm thick dielectric layer Si<sub>3</sub>N<sub>4</sub> (dielectric constant 7) is mounted on the signal deck.

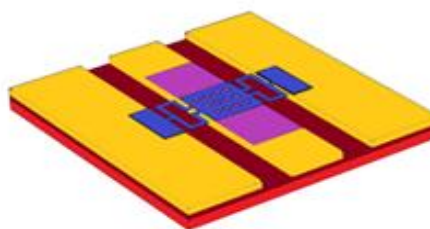


Fig.1. The proposed switch design.

**Table 1: Dimensions of the Proposed Switch**

| Switch Parameters                   | Shunt Switch |
|-------------------------------------|--------------|
| 1. Spring Constant                  | 9.83 N/m     |
| 2. Pull-in-voltage                  | 16.22 volts  |
| 3. Switching time                   | 31.2 $\mu$ s |
| 4. Upstate Capacitance              | 7.38 pF      |
| 5. Downstate Capacitance            | 6.99 pF      |
| 6. Downstate to Upstate Capacitance | 58.948       |

**Table 2:**

| Structural Element                  | Dimension( $\mu$ m) |
|-------------------------------------|---------------------|
| 1. Substrate thickness              | 20.0                |
| 2. Ground and Signal line thickness | 15.0                |
| 3. Dielectric layer thickness       | 0.1                 |
| 4. Oxide layer thickness            | 300.0               |
| 5. Bridge Length                    | 100.0               |
| 6. Bridge Width                     | 1.0                 |
| 7. Bridge Thickness                 | 10.0                |
| 8. Air gap                          | 2.0                 |

**SWITCH PARAMETERS**
**Spring constant:**

The spring is constant for shunting without residual pressure

$$k = 32Ew\left(\frac{t}{l}\right)^3$$

The spring constant for a fixed beam with residual pressure

$$k = 32Ew\left(\frac{t}{l}\right)^3 + 8\sigma(1 - \nu)w\left(\frac{t}{l}\right)$$

The membrane is fixed for the series switch, at one end there is no residual stress. Where

$\sigma$ =biaxial residual stress (Pa)

$\nu$  = Poisson's ratio

w=beam width

W= width of the signal line under the beam.

**Actuation Voltage:**

It is calculated by using below equation

$$V_p = \sqrt{\frac{8kg_0^3}{27\varepsilon_0 Ww}}$$

Here  $g_0$ =Air gap

$\varepsilon_0$ =free space permittivity.

**Mechanical resonant frequency:**

The resonance frequency is determined by a mechanical Spring.

$$\omega_0 = \sqrt{\frac{k}{m}}$$

**Switching time:**

The time it takes to move from ON to OFF is time and Vice versa.

$$T_s = \frac{3.67V_p}{V_s\omega_0}$$

Where  $V_p$ =pull-in voltage

$$V_s = \text{Supply voltage, } V_s = 1.4 V_p$$

**Up-state capacitance (Con):**

The shunt shift is demonstrated by two short sections of the line and a lumped template. The Upstate Capacity Con is determined as

$$C_{on} = \frac{\varepsilon_0 W \omega}{g + \frac{t_d}{\varepsilon_r}}$$

Where,  $t_d$ = Dielectric layer thickness.

The coefficient of reflection in the upward state is given by

$$S_{11} = \frac{-j\omega C_{on} Z_0}{2 + j\omega C_{on} Z_0}$$

The frequency of resonance is determined

$$f_0 = \frac{1}{2\pi\sqrt{LC_{on}}}$$

**Down-state capacitance ( $C_{off}$ ):**

The capacitance downstairs can be measured as

$$C_{off} = \frac{\varepsilon_0 \varepsilon_r W \omega}{t_d}$$

**Capacitance Ratio ( $C_{ratio}$ ):**

The ratio of two capacitances is given by.

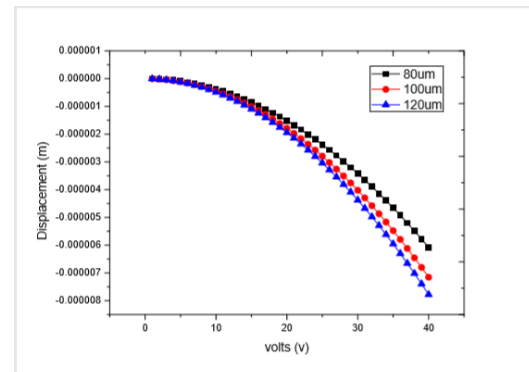
$$C_{ratio} = \frac{C_{off}}{C_{on}}$$

**RESULTS AND DISCUSSION**
**Electromechanical analysis of capacitive series switch:**

It was planned and simulated in COMSOL in order to analyze Effect on the switch output of geometric parameters. In this case we took the mathematical parameters beam width and length, air gap, driver and dielectric materials. Each parameter varies from one parameter to another.

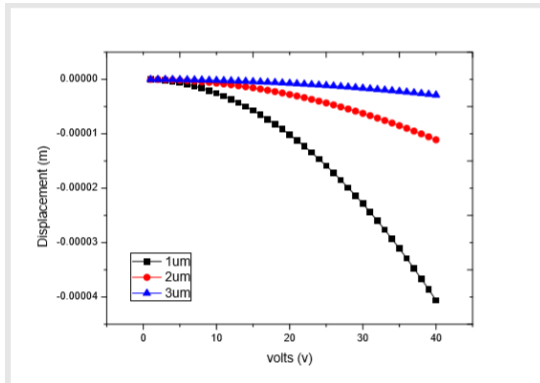
**Effect of beam width:**

Figure below displays the displacement graphs of various beam width values for a fixed length and thickness of the beam value. As the pull-in voltage inverts pull-in voltage to the width of the beam. The 120  $\mu$ m light has a lower voltage than 80 and 100  $\mu$ m, respectively. So, we picked 120  $\mu$ m powder diameter.


**Fig.2. Multi Beam size characteristics displacement map**

**Effect of Air gap:**

The diagrams shown below show a number of air gaps for displacement. The displacement is measured by a varying air gap of 3 to 1  $\mu\text{m}$ . The voltage required is reduced when air gap decreases. Nevertheless, less air gap is not predictive in terms of manufacturing.



**Fig.3. Specific Air gap values displacement map.**

**Effect of beam thickness:**

As shown in figure, the effect on the actuator voltage of the beam thickness. It is clear that the actuation voltage often decreases with decreased beam size. The light with a voltage of 0.5  $\mu\text{m}$  is less than 1 and 1.5  $\mu\text{m}$ .

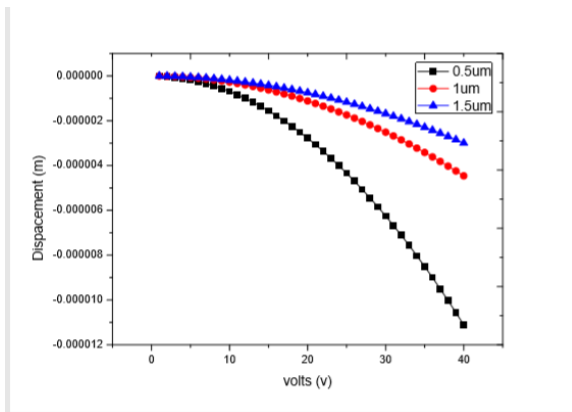


**Fig.4 Different beam thickness values displacement graphs.**

**Effect of dielectric material:**

The right conductor and dielectric material should be selected to obtain the best output of the switch. The best displacement for smaller voltage is shown among the three conductors selected in gold.

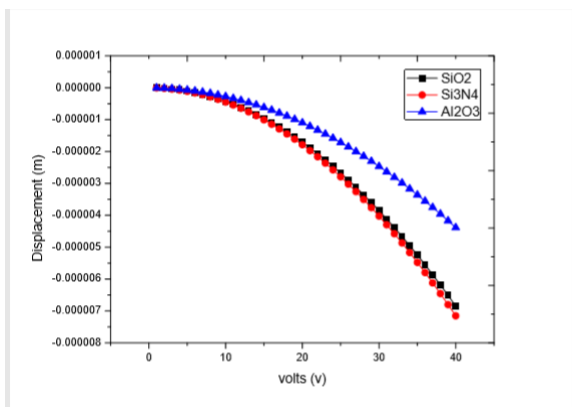


**Fig.5. Shift diagrams of different materials of the dielectric.**

**Effect of Conductor:**

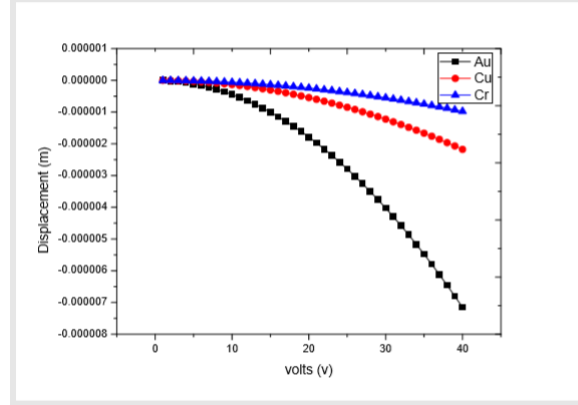


**Fig.6. Shift diagrams of different materials of the conductor.**

**Switching time analysis:**

The time to switch is  $V_p, V_s$  and  $w_0$  of the formula shift (4). As shown in figure 8, the measurement of voltage vs time of switching is. The switching time is 36.64  $\mu\text{s}$  at the pull-in voltage i.e. 18.89.

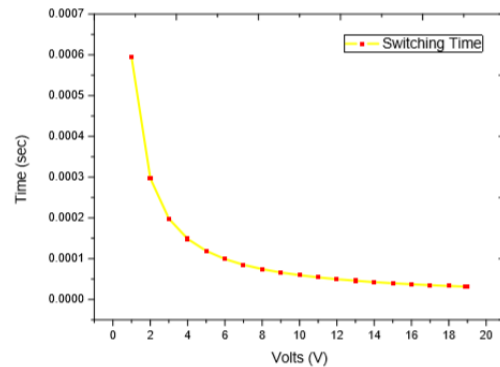


**Fig.7. Time to spring voltage switching.**

**Capacitive research up and downstate:**

The power ratio is an example of the potential gap between the two switching states. The dielectric thickness and the relative permittivity of the beam region are conveyed to system capacitance. From the fig. from the fig. received the upstate 40.9fF capacitance and the down state 4.45 pF capacitance. This gives us 108.69 power ratio.

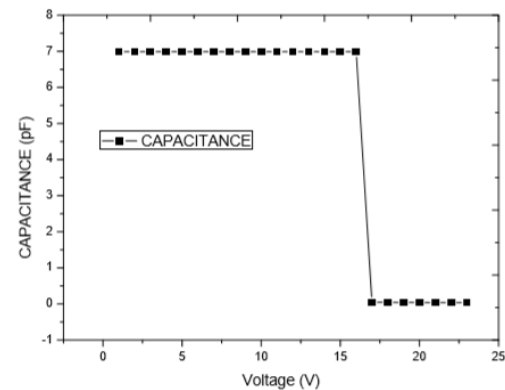


**Fig.8 Capacity vs voltage curve shunt shift**

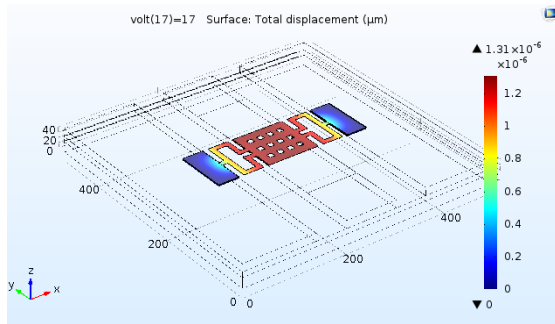


Fig.9. Beam deflection

#### Capacitive Shunt Shift Electromagnetic Analysis:

The performance assessment of the radio frequency is carried out by using HFSS technology. Insert return and isolation are key parameters for validating the switch performance for the device to be assessed. In the middle of the top and bottom electrode, the air gap persists at a length of 3  $\mu\text{m}$ . From 0 to 10 GHz frequency range measured.

#### Return Loss (ON-State):

The simulation electromagnetic is conducted from 0-10 GHz and parameters are analyzed. The return loss in ON condition is observed from the figure in the range of -5-35 dB. Eleven. Fig shows a good insertion loss of -0.01-0.5 dB in ON condition.

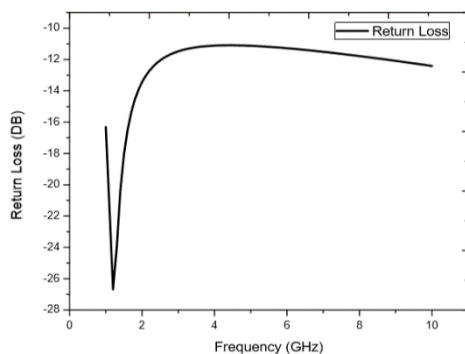


Fig.10. Shunt change return loss in its ON condition.

#### Return Loss (OFF-State):

OFF return loss is in the range of 1-15 dB, as shown by the OFF isolation in the range of -1-11 dB. The consequence is the OFF condition.

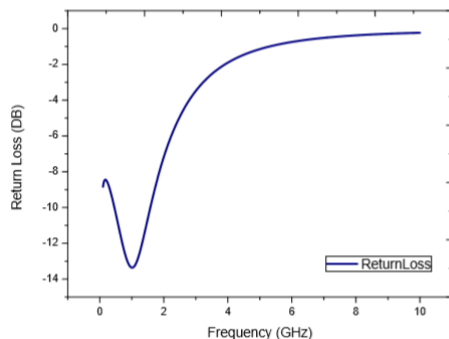


Fig.11. Shunt change return loss in its OFF condition.

#### Isolation Loss (OFF- State):

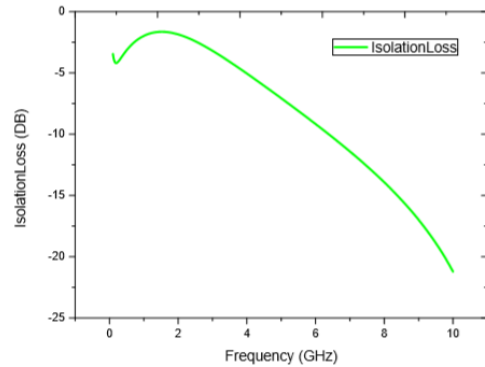


Fig.12. Shunt change isolation loss in its OFF condition.

#### Insertion (ON-State):

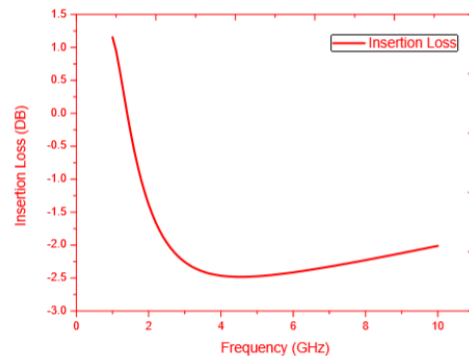


Fig.13. Shunt change insertion loss in its ON condition.

#### CONCLUSION:

In this article a RF MEMS shunt model is provided to evaluate electromechanical and electromagnetic parameters. The actuation voltage of the virtual switch is 32V. The ON status indicates a return loss of -35 dB at 10GHz and a decrease of -0.1 dB at 10 GHz as shown in the graphs. The insulation is above -11 dB at 10 GHz for the change in the OFF state (S21). The switch's power ratio is relatively high at 108.69. The switch has outstanding RF properties. In tunable filter applications it is extremely useful.

#### REFERENCES:

1. Rebeiz G.M., " RF MEMS Theory, Design and Technology," Wiley, New Jersey, 2003.
2. K. Rangra, et al., " Symmetric toggle switch - a new type of rf MEMS switch for telecommunication applications: design and fabrication," Sens. Actuators A: Phys 123-124, pp.505-514,2005.
3. M. Angira, et al., " Design and investigation of a low insertion loss, broadband enhanced self and hold down power RF-MEMS switch," Microsyst. Technol. vol.21 1173-1178,2015.
4. F. Giacomozzi, et al., " Development of high con/coff ratio RF MEMS shunt switches," Rom. J. Inf. Sci.Tech. vol.11,143-151.2008.
5. M. Tanga, et al., " High isolation X-band MEMS capacitive switches, J. Sensors and Actuators," A 120 ,241-248,2005.
6. K.J. Rangra et al., Electrostatic low actuation voltage RF MEMS switches for telecommunications (Ph.D. thesis), Department of Information Technology, University of Trento, Trento, 2005.
7. M. Angira, et al., " A novel interdigitated, inductively tuned, capacitive shunt RF-MEMS switch for X and K bands applications," in: Proceedings of NEMS, Hawaii, pp. 139-142, USA, 2014.